Reconstructing the Past from Imprecise Knowledge of the Present: Some Examples of Non Uniqueness in Solving Parabolic Equations Backward in Time

Alfred S. Carasso

Reconstructing the Past from Imprecise Knowledge of the Present: Some Examples of Non Uniqueness in Solving Parabolic Equations Backward in Time

Alfred S. Carasso
Applied and Computational Mathematics Division
Information Technology Laboratory

April 2011

RECONSTRUCTING THE PAST FROM IMPRECISE KNOWLEDGE OF THE PRESENT: SOME EXAMPLES OF NON UNIQUENESS IN SOLVING PARABOLIC EQUATIONS BACKWARD IN TIME

ALFRED S. CARASSO*

Abstract. Identifying sources of ground water pollution, and deblurring astronomical galaxy images, are two important applications generating growing interest in the numerical computation of parabolic equations backward in time. However, while backward uniqueness typically prevails in parabolic equations, the precise data needed for the existence of a particular backward solution is seldom available. This paper discusses previously unexplored non uniqueness issues, originating from trying to reconstruct a particular solution from imprecise data. Explicit 1D examples of linear and nonlinear parabolic equations are presented, in which there is strong computational evidence for the *existence* of distinct solutions $w^{red}(x,t)$ and $w^{green}(x,t)$, on $0 \leq t \leq 1$. These solutions have the property that the traces $w^{red}(x,1)$ and $w^{green}(x,1)$ at time $t = 1$, are close enough to be visually indistinguishable, while the corresponding initial values $w^{red}(x,0)$ and $w^{green}(x,0)$, are vastly different, well-behaved, physically plausible functions, with comparable L^2 norms. This implies effective non uniqueness in the recovery of $w^{red}(x,0)$ from approximate data for $w^{red}(x,1)$. In all these examples, the Van Cittert iterative procedure is used as a tool to discover unsuspected, valid, additional solutions $w^{green}(x,0)$. This methodology can generate numerous other examples and indicates that multidimensional problems are likely to be a rich source of striking non uniqueness phenomena.

Key words. advection dispersion equation; backward parabolic equations; hydrologic inversion; image deblurring; ill-posed continuation; non uniqueness; Van Cittert iteration.

AMS subject classifications. 35R25, 35B60, 35K10, 65M20, 65M30.

1. Introduction. This paper discusses computationally generated 1D examples of non uniqueness in solving parabolic equations backward in time. These examples are unexpected and, to the author's knowledge, are of a type not previously known in the literature. Such non uniqueness is of major significance in applications. Resolving the increased uncertainty in backward reconstructions may require more detailed prior information about the true solution than may be available. The methodology used to create these examples can generate numerous other examples. Multidimensional problems are likely to be a rich source of striking non uniqueness phenomena. As noted below, backward uniqueness typically prevails in parabolic equations. However, the precise data needed for the existence of a particular backward solution is seldom available. The non uniqueness issues discussed here originate from trying to reconstruct a particular solution from imprecise data.

There has been growing interest in recent years in the development of numerical methods for solving parabolic equations backward in time. In [2], [9], [10], [16], [19], [23], [24], [26], [28], and [32], various useful methods are analyzed and illustrated with interesting test computations. Currently, the two most significant areas of application of backward parabolic equations are *hydrologic inversion* and *image deblurring*. In hydrologic inversion, the aim is to identify sources of groundwater pollution by reconstructing the contaminant plume history. This involves solving the advection dispersion equation (ADE) backward in time, given the contaminant spatial distribu-

tion $g(x, y)$ at the current time T,

$$C_t = \nabla.\{D\nabla C\} - \nabla.\{vC\}, \qquad 0 < t \le T,$$

(1)

$$C(x, y, T) = g(x, y).$$

Here, C is the mass concentration, D is the diffusion tensor, and v is the velocity vector. There is a large literature on this topic. Instructive expository discussions of this problem, together with backward calculations of realistic examples, principally in 1D, may be found in [3], [4], [5], [6], [7], [25], [29], and [31].

Brownian motion is pervasive in many branches of science, including image science. For this reason, images blurred by Gaussian point spread functions are a common occurrence. Deblurring Gaussian blur is mathematically equivalent to solving the heat conduction equation backward in time, with the noisy blurred image $g(x, y)$ as data at time $t = 1$, and with conduction coefficient $\alpha > 0$ proportional to the point spread variance,

$$w_t = \alpha \Delta w, \qquad 0 < t \le 1,$$

(2)

$$w(x, y, 1) = g(x, y).$$

A discussion of this problem may be found in [11], [12], [15], [17], [27], and [33]. In many areas of applied science, the underlying random process involves a fundamental modification of Brownian motion, whereby the motion takes place in a specific randomized operational time $Q(t)$, rather than in standard clock time t. This new *subordinated* Brownian process leads to non standard diffusion equations. Such notions have also been found useful in image deblurring. In [14], and references therein, backward in time problems for fractional and/or logarithmic diffusion equations,

$$(3) \qquad w_t = -\alpha(-\Delta)^\beta w, \qquad w_t = -\left[\lambda \log\{1 + \gamma(-\Delta)^\beta\}\right] w, \qquad 0 < t \le 1,$$

are successfully applied, in a blind deconvolution scheme, to enhance Hubble Space Telescope images, as well as Scanning Electron Microscope images of interest in Nanotechnology. In (3), α, β, λ, and γ are positive constants, with $\beta < 1$.

2. Stabilized problems, backward uniqueness, and stability estimates. Theoretical discussions of backward parabolic equations and other non standard problems may be found in [1], [13], [20], [21], [30], and the references therein. Backward parabolic equations are classical examples of ill-posed problems in the sense of Hadamard. Typically, a backward solution exists only for highly restricted data satisfying certain smoothness and other requirements that are not easily characterized. In most cases of practical interest, when a solution exists, it is unique. However, backward solutions depend discontinuously on the data for which they exist and slight changes in that data can result in very large, if not explosive, changes in the corresponding solutions.

Backward parabolic problems can be stabilized by prescribing an a-priori bound M for the L^2 norm of the solution at time $t = 0$. The following situation illustrates the general ideas. Let Ω be a bounded domain in R^n with smooth boundary $\partial\Omega$. Let L be an elliptic operator in Ω acting on smoothly differentiable functions vanishing on $\partial\Omega$. In the simplest case, L is a linear positive self adjoint differential operator with variable coefficients that may depend on time. However, we will also consider nonlinear problems. In all cases, the forward problem $w_t = Lw, \; t > 0$, is well-posed.

The stabilized backward parabolic problem for L may be stated as follows. Given $f(x) \in L^2(\Omega)$ and M, $\delta > 0$, with $\delta \ll M$, find all solutions of

$$(4) \qquad w_t = Lw, \quad x \in \Omega, \qquad w = 0, \ x \in \partial\Omega, \qquad 0 < t \leq T,$$

such that

$$(5) \qquad \| w(.,T) - f \|_2 \leq \delta, \qquad \| w(.,0) \|_2 \leq M.$$

It is assumed that $f(x)$, δ, and M are compatible with the existence of solutions. Here, $f(x)$ is presumed to be a sufficiently close L^2 approximation to the exact values $w(x,T)$ at $t = T$, of a solution $w(x,t)$ of (4), believed to satisfy $\| w(.,0) \|_2 \leq M$. In many engineering or applied science contexts, only educated guesses would generally be available to estimate δ and M, rather than exact values. Typically, the L^2 relative error

$$(6) \qquad \| w(.,T) - f \|_2 \ / \ \| w(.,T) \|_2 \leq \delta / \{\| f \|_2 - \delta\} \approx \delta / \| f \|_2,$$

might be expected to be on the order of 1% or thereabouts. Since the given data $f(x)$ may simultaneously approximate several distinct solutions $w^p(x,t)$ of (4) at time T, there are, in general, infinitely many possible solutions of (4) and (5). If δ is small, it is generally assumed that any two such solutions would differ only slightly. The extent to which this expectation is justified is determined by the backward stability inequality governing the particular parabolic equation $w_t = Lw$.

The following *logarithmic convexity* method, [1], [20], [30], is often used to obtain stability inequalities for ill-posed continuation problems. Let $w^1(x,t)$ and $w^2(x,t)$ be any two solutions of the well-posed forward problem $w_t = Lw$. For $0 \leq t \leq T$, let $F(t) = \| w^1(.,t) - w^2(.,t) \|_2^2$. Using properties of the differential operator L, together with appropriate restrictions on the class of solutions being considered, the aim is to establish the following inequality

$$(7) \qquad F(t)F''(t) - \{F'(t)\}^2 \geq -a_1 \ F(t)F'(t) - a_2 \ F^2(t), \qquad 0 < t < T,$$

where a_1 and a_2 are constants.

If $a_1 = a_2 = 0$ in (7), then $\log F(t)$ is a convex function of t and

$$(8) \qquad F(t) \leq \{F(0)\}^{(T-t)/T} \{F(T)\}^{t/T}, \qquad 0 \leq t \leq T.$$

More typically, $a_1 \neq 0$ in (7). In that case, let

$$(9) \qquad q = -a_2/2a_1, \qquad \mu(t) = \{e^{-a_1 t} - 1\}\{e^{-a_1 T} - 1\}^{-1}, \qquad 0 \leq t \leq T.$$

Then, as shown in [1], [20], [30],

$$(10) \qquad e^{2qt} F(t) \leq \{F(0)\}^{1-\mu(t)} \{e^{2qT} F(T)\}^{\mu(t)}, \qquad 0 \leq t \leq T.$$

Inequalities of this type have been obtained for a wide class of problems, in addition to the class of parabolic problems $w_t = Lw$ considered in this paper; see [1], [13], [20], [21], [30]. For solutions satisfying a prescribed L^2 bound M at $t = 0$, we obtain from (10), for $0 \leq t \leq T$,

$$(11) \quad e^{qt} \| w^1(.,t) - w^2(.,t) \|_2 \leq \{2M\}^{1-\mu(t)} \{e^{qT} \| w^1(.,T) - w^2(.,T) \|_2\}^{\mu(t)}.$$

This inequality establishes L^2 Hölder-continuous dependence of solutions at any fixed t with $0 < t \leq T$, on the data at time T. The Hölder exponent $\mu(t)$ satisfies $0 \leq \mu(t) \leq 1$, with $\mu(t) > 0$, $t > 0$, $\mu(T) = 1$, $\mu(0) = 0$, and $\mu(t) \downarrow 0$ monotonically as $t \downarrow 0$.

2.1. Backward uniqueness. The inequality (11) implies backward uniqueness of solutions satisfying a prescribed bound. Indeed, if $\| w^1(.,T) - w^2(.,T) \|_2 = 0$, then $\| w^1(.,t) - w^2(.,t) \|_2 = 0$ for every $0 < t \leq T$, since $\mu(t) > 0$ for $t > 0$. By continuity, $\| w^1(.,t) - w^2(.,t) \|_2 = 0$ on $0 \leq t \leq T$.

Remarkably, backward uniqueness even holds true for the Navier-Stokes equations. This landmark result was obtained in [21] by establishing the stability inequality (10) appropriate for these equations.

2.2. Backward continuity. We may now address the recoverability of solutions in the stabilized backward problem (4), (5). Let $w^1(x,t), w^2(x,t)$ be any two possible solutions of (4), (5). Then,

$$(12) \qquad \| w^1(.,0) - w^2(.,0) \|_2 \leq 2M, \qquad \| w^1(.,T) - w^2(.,T) \|_2 \leq 2\delta.$$

Hence, from (11),

$$(13) \qquad e^{qt} \| w^1(.,t) - w^2(.,t) \|_2 \leq 2M^{1-\mu(t)} \{ e^{qT}\delta \}^{\mu(t)}, \qquad 0 \leq t \leq T.$$

Here, the dependence of the Hölder exponent $\mu(t)$ on t plays a crucial role. In the best possible case, that of a linear self adjoint elliptic operator L with time-independent coefficients, we have $\mu(t) = t/T$, so that $\mu(t)$ decays linearly to zero as continuation progresses from $t = T$ to $t = 0$. At $t = T/2$, we have $\mu(T/2) = 1/2$ and, assuming $q = 0$, $\| w^1(.,T/2) - w^2(.,T/2) \|_2 \leq 2\sqrt{M\delta}$. This loss of acccuracy from $O(\delta)$ to $O(\sqrt{\delta})$, while still only half way to $t = 0$, is noteworthy. More typically, with $a_1 < 0$ in (7), $\mu(t)$ is *sublinear* in t, possibly with rapid exponential decay. This can lead to much more severe loss of accuracy as reconstruction progresses to $t = 0$. As shown in [13], rapid decay of μ to zero can be brought about by various factors, including nonlinearity, non self adjointness, diffusion coefficients that grow rapidly with time, or adverse spectral properties in the elliptic operator L. In all cases, (13) does not guarantee any accuracy at $t = 0$, but only provides the redundant information $\| w^1(.,0) - w^2(.,0) \|_2 \leq 2M$.

While inequality (13) is best-possible in general, it necessarily contemplates worst case scenarios that may be too pessimistic in some applications. Indeed, successful recoveries of contaminant plumes in hydrology, as well as striking enhancement of Hubble telescope galaxy images, have been documented [5], [6], [14]. Nevertheless, the behavior of the Hölder exponents in (13) reflects a basic underlying truth. This behavior is indicative of the rate at which the particular evolution equation $w_t = Lw$ has forgotten the past and, hence, of the subsequent difficulty of reconstructing the past from imperfect knowledge of the present. This paper illuminates this deeper meaning by exhibiting specific 1D parabolic equations on $0 \leq t \leq 1$, with distinct solutions $w^{red}(x,t)$ and $w^{green}(x,t)$. These solutions are such that their traces at $t = 1$, $w^{red}(x,1)$, $w^{green}(x,1)$, are visually indistinguishable, while their corresponding initial values $w^{red}(x,0)$, $w^{green}(x,0)$, are vastly different. Therein lies the difficulty of reconstructing the correct backward solution from approximate data at $t = 1$.

3. Exploring backward solutions using Van Cittert iterations. Consider the well-posed, forward, linear or nonlinear parabolic initial value problem $w_t = Lw$, $0 < t \leq 1$, $w(x,0) = w_0^{red}(x)$. Define S to be the associated solution operator at time $t = 1$. Thus, given any $h(x)$ in $L^2(\Omega)$, the operator S uses $h(x)$ as initial data $w(x,0)$ in (4) and produces the corresponding solution $w_h(x,1)$ at $t = 1$, so that $S[h(x)] = w_h(x,1)$. In particular, $S[w_0^{red}(x)] = w^{red}(x,1)$. Next, let $f(x)$ be an approximation to $w^{red}(x,1)$ with $\| w^{red}(.,1) - f \|_2 \leq \delta$, as in (5). With fixed

relaxation parameter $\gamma > 0$, and with $h^1(x) = \gamma f(x)$, consider the following iterative procedure

$$(14) \qquad h^{n+1}(x) = h^n(x) + \gamma \left\{ f(x) - S[h^n(x)] \right\}, \qquad n \geq 1.$$

In spectroscopy and image processing, with S an explicitly known linear convolution integral operator, this procedure is the widely used Van Cittert iteration [18], [22]. In these applications, the Van Cittert method generally produces useful results after finitely many iterations, although it may not converge. In the present case, S may be highly nonlinear and is not known explicitly. For given $h(x)$ in $L^2(\Omega)$, $S[h(x)]$ must be obtained by numerically solving the well-posed forward parabolic problem.

Clearly, in the present parabolic context, the Van Cittert iteration is unlikely to converge. Indeed, if $h^n \to h^\dagger$ in $L^2(\Omega)$ in (14), then $S[h^\dagger(x)] = f(x)$. However, $S[h^\dagger(x)]$ necessarily satisfies highly restrictive smoothness requirements and these are not likely to be met by the given approximate data $f(x)$. Nevertheless, as will be seen below, the Van Cittert iteration is a valuable exploratory tool. In a wide variety of 1D linear and nonlinear parabolic equations, this procedure typically generates iterates $h^n(x)$ such that the L^∞ norm of the residual, $\| f - S[h^n] \|_\infty$, decays quasi monotonically to a small value after finitely many iterations. This is often sufficient for our purpose. From (5), if for some positive integer N we find $\| f - S[h^N] \|_2 \leq \delta$, with $\| h^N \|_2 \leq M$, then $h^N(x)$ is a valid candidate reconstruction of $w^{red}(x, 0)$, given the approximation $f(x)$ to the unavailable $w^{red}(x, 1)$.

4. Numerical implementation of Van Cittert's iteration. All of the examples discussed below are one dimensional, take place on the interval $-1 \leq x \leq 1$, involve smooth coefficients and initial values, and have homogeneous Dirichlet boundary conditions. To implement the iterative process in (14), use is made of an efficient, highly accurate parabolic equation solver. This method of lines procedure is discussed in [8] and is implemented as subroutine *D03PDF/D03PDA* in the NAG Mathematical Software Library. It uses Chebyshev C^0 collocation for spatial differencing, together with backward time differencing to advance the solution forward in time. Here, one hundred equispaced breakpoints, $-1 = x_1 < x_2 < x_3 < \cdots < x_{100} = 1$, are placed on $[-1, 1]$. Between each pair of breakpoints, the solution of $w_t = Lw$ is approximated by a cubic Chebyshev polynomial whose space and time derivatives are made to satisfy the parabolic equation at two collocation points chosen internally by the subroutine. C^0 continuity is enforced at the breakpoints. This leads to a total of 298 (non equispaced) mesh points on $[-1, 1]$. For each $t_k = k\Delta t$, the computed solution $w(x, t_k)$ is a piecewise cubic polynomial in x on $[-1, 1]$.

All the examples below will follow the same road map. With initial data $w_0^{red}(x)$, the parabolic problem $w_t = Lw$ is first integrated up to time $t = 1$, to produce a presumed good approximation $f(x)$ to the unknown true solution $w^{red}(x, 1)$. This calculated $f(x)$, shown as a black curve in the figures, is then viewed as given data in an applied science or engineering context and is used in the Van Cittert procedure (14) to recover the unknown initial value $w_f(x, 0)$ that gave rise to $f(x)$ at $t = 1$. However, it will turn out that $f(x)$ is also a close approximation to an unsuspected additional solution $w^{green}(x, 1)$ corresponding to initial data $w_0^{green}(x)$ that can be vastly different from $w_0^{red}(x)$. The relaxation parameter γ in (14) was set to 0.5 in all six examples.

5. Example 1 (Fig. 1). Linear self adjoint. The following relatively well-behaved example is used to set the stage for the less well-behaved examples to follow.

Mild backward non uniqueness in Example 1
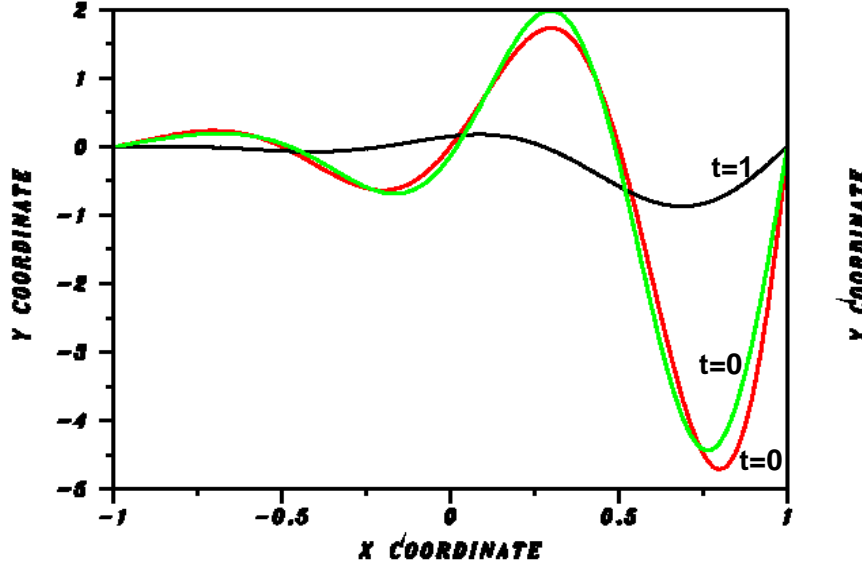
**Either red or green initial values at t=0, terminate on black curve
at t=1 to within 3.1E−3 pointwise, and L2 relative error=4.1E−3.**

FIG. 1. *Well-behaved self adjoint problem. Data $f(x)$ (black curve), approximating solution $w^{red}(x,t)$ at time $t = 1$ with an L^2 relative error of 0.41%, recovers reasonably close initial value $w_0^{green}(x)$, in lieu of true initial value $w_0^{red}(x)$.*

With $a = 0.05$, $\alpha = 0.05$, $\sigma = 0.025$, consider the linear, self adjoint, variable coefficient problem

$$w_t = a \left\{ e^{(\sigma x + \alpha t)} w_x \right\}_x, \quad -1 < x < 1, \quad 0 < t \leq 1.0,$$
(15)
$$w(x,0) = e^{2x} \sin(2\pi x), \quad -1 \leq x \leq 1, \quad w(-1,t) = w(1,t) = 0, \quad t \geq 0.$$

The initial data in (15), denoted by $w_0^{red}(x)$, is shown as the red trace in Figure 1. Using the parabolic solver in Section 4, the computed solution at time $t = 1$, denoted by $f(x)$, is shown as the black trace in Figure 1. While that computed solution is, in fact, an excellent approximation, we view $f(x)$ as merely a good approximation to the unknown true solution $w^{red}(x,1)$ with $\| w^{red}(.,1) - f \|_2 \leq \delta$. We stress that in an actual engineering application with real data, the expected L^2 relative error $\delta / \| f \|_2$ might be on the order of 1% or thereabouts. Using $f(x)$ in the Van Cittert procedure (14), we seek to recover the unknown initial values $w_f(x,0)$ that gave rise to $f(x)$ at $t = 1$. For each successive iterate $h^n(x)$ in (14), we can evaluate and monitor the L^∞ residual, $\| f - S[h^n] \|_\infty$, as well as the L^2 relative error at $t = 1$, $\| f - S[h^n] \|_2 / \| f \|_2$. In this example, these two errors decay monotonically.

After 200 iterations, the L^∞ residual is 3.1E-3, so that the trace of $S[h^{200}](x)$ is visually indistinguishable from that of $f(x)$, while the L^2 relative error at $t = 1$ is 0.4%. The iterate $h^{200}(x)$ is shown as the green trace $w_0^{green}(x)$ in Figure 1. Moreover, $\| w_0^{red} \|_2 = 1.8$, while $\| w_0^{green} \|_2 = 1.7$. Therefore, both solutions $w^{red}(x,t)$ and

## Behavior of Van Cittert residual norm in Example 2
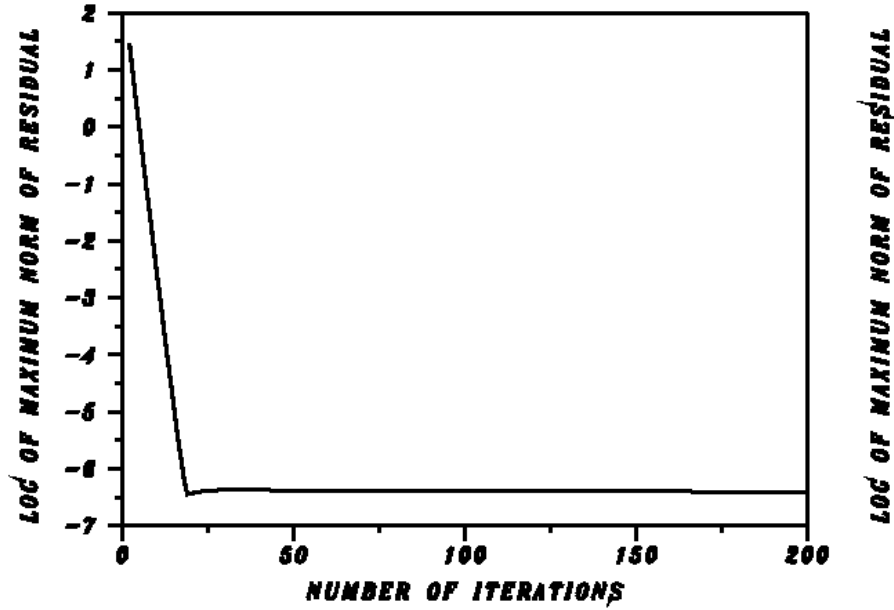
Effective backward non uniqueness in Example 2
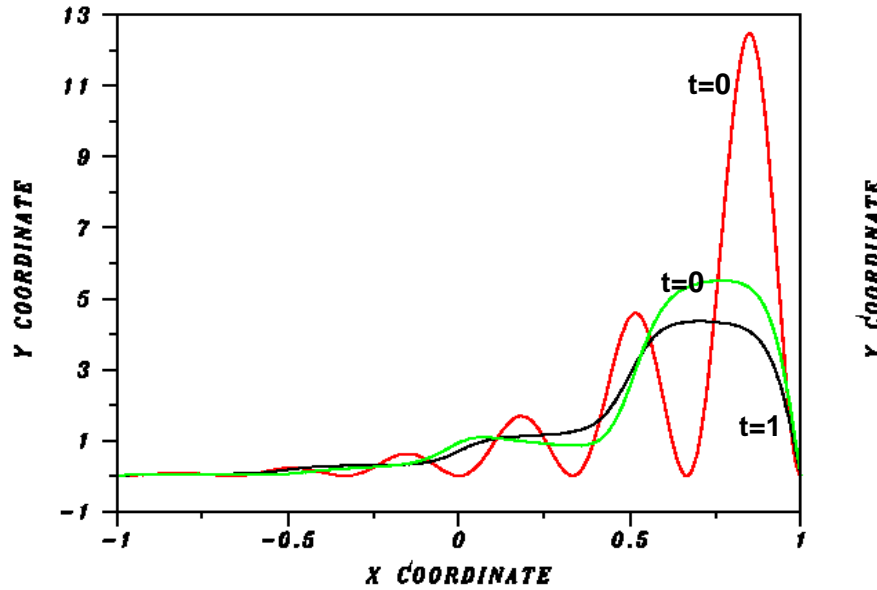
**Either red or green initial values at t=0, terminate on black curve
at t=1 to within 1.4 E−3 pointwise, and L2 relative error=2.3E−4.**

FIG. 2. *TOP. Behavior of $\log \{\| f - S[h^n] \|_\infty\}$ versus iteration number n, in Van Cittert procedure in Example 2. BOTTOM. Ill behavior in non self adjoint problem. Accurate data $f(x)$ (black curve), approximating solution $w^{red}(x,t)$ at time $t = 1$ with an L^2 relative error of 0.023%, recovers vastly different initial value $w_0^{green}(x)$, in lieu of true initial value $w_0^{red}(x)$.*

Red and green traces at t=1 coincide in Example 2
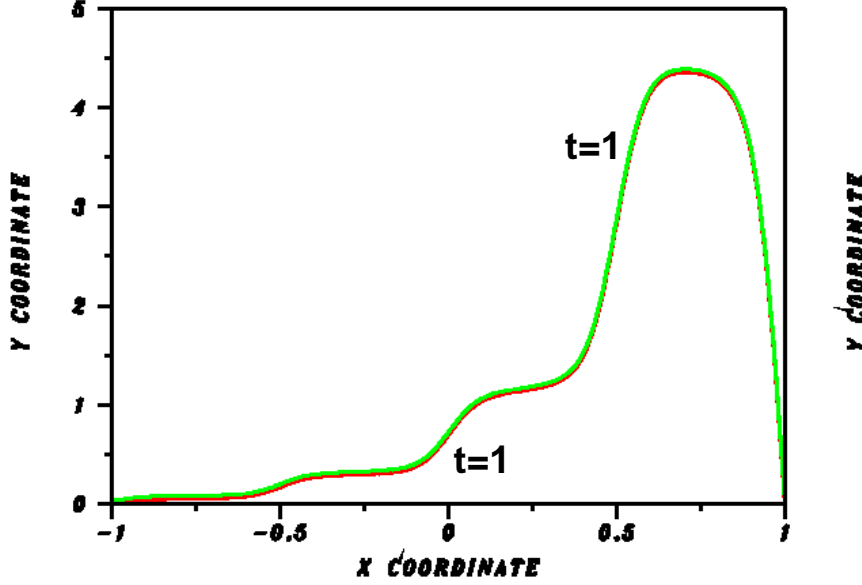
Green trace artificially raised to render red trace visible.

FIG. 3. *Red and green traces are the solutions at time $t = 1$, $w^{red}(x, 1)$, $w^{green}(x, 1)$, corresponding to the initial values $w_0^{red}(x)$, $w_0^{green}(x)$, in Figure 2 (bottom). Traces at $t = 1$ agree to within $1.43E - 3$, pointwise. This close agreement explains the difficulty of recovering $w_0^{red}(x)$ from approximate values for $w^{red}(x, 1)$ in Example 2.*

$w^{green}(x, t)$ satisfy

$$(16) \qquad \| w(., 1) - f \|_2 \leq \delta \leq 0.004 \| f \|_2, \qquad \| w(., 0) \|_2 \leq M = 1.8.$$

Thus, given only the approximate data $f(x)$, $w_0^{green}(x)$ in Figure 1 can be considered a valid reconstruction of the unknown initial data. Evidently, $f(x)$ is a close approximation to (at least) two distinct true solutions at $t = 1$, $w^{red}(x, 1)$ and $w^{green}(x, 1)$. These two solutions have visually indistinguishable traces at $t = 1$, but have distinct traces at $t = 0$. In this example, either reconstruction at $t = 0$ might be considered successful.

The next two examples offer a sharp contrast to the mild non uniqueness behavior in the above self adjoint problem.

6. Example 2 (Figs. 2 and 3). Linear non self adjoint. With $a = 0.05$, $\alpha = 0.05$, $\sigma = 0.025$, this example involves a linear non self adjoint equation with variable coefficients, non negative initial values, and non negative solution,

$$(17) \qquad w_t = a \left\{ e^{(\sigma x + \alpha t)} w_x \right\}_x + \left\{ \sin(4\pi x) \right\} w_x, \quad -1 < x < 1, \ \ 0 < t \leq 1.0,$$

$$w(x, 0) = e^{3x} \sin^2(3\pi x), \quad -1 \leq x \leq 1, \ \ w(-1, t) = w(1, t) = 0, \ \ t \geq 0.$$

The initial data in (17), denoted by $w_0^{red}(x)$, is shown as the red trace in Figure 2 (bottom) while the computed approximation $f(x)$ to $w^{red}(x, 1)$ is shown as the black

trace in the same figure. Using $f(x)$ in (14), the Van Cittert procedure was applied for 1000 iterations and resulted in $h^{1000}(x) = w_0^{green}(x)$, shown as the green trace in Figure 2 (bottom), with a final L^∞ residual of 1.4E-3, and an L^2 relative error at $t = 1$, $\| f - S[h^{1000}] \|_2 / \| f \|_2 = 0.023\%$. Both of these values are noticeably smaller than was the case in Example 1. Moreover, $\| w_0^{red} \|_2 = 3.3$, while $\| w_0^{green} \|_2 = 2.4$. Therefore, both solutions $w^{red}(x, t)$ and $w^{green}(x, t)$ satisfy

(18) $\| w(., 1) - f \|_2 \leq \delta \leq 0.00023 \| f \|_2,$ $\| w(., 0) \|_2 \leq M = 3.3.$

Clearly, $w_0^{green}(x)$ is a valid reconstruction of the initial data corresponding to the given data $f(x)$ at $t = 1$. The behavior of $\log \{\| f - S[h^n] \|_\infty\}$ versus n, is shown in Figure 2 (top) for the first 200 iterations. Evidently, the iterative procedure locked onto $w_0^{green}(x)$ after twenty or so iterations, with very slow systematic decrease in the L^∞ residual norm taking place thereafter.

The traces for $w^{red}(x, 1)$ and $w^{green}(x, 1)$ are plotted in Figure 3 and are visually indistinguishable. In fact, in Figure 3, the green trace was artificially raised by 0.05, so as to render the red trace visible. Both these traces coincide with the black trace in Figure 2 (bottom). Evidently, the given data $f(x)$ is a close approximation to two very distinct solutions of the parabolic problem in (17) and this is a good example of effective backward non uniqueness. Indeed, given the black trace in Figure 2, $w_0^{green}(x)$ would appear to be a more likely initial value than $w_0^{red}(x)$. In ill-posed inverse problem computations, smoothness and non negativity of solutions are considered beneficial regularizing constraints. Here, both traces are smooth and non negative, but a serious ambiguity remains.

7. Example 3 (Figs. 4 and 5). Linear non self adjoint. This example differs from the preceding one only by having a different coefficient multiplying the w_x term. With $a = 0.05$, $\alpha = 0.05$, $\sigma = 0.025$, consider

(19)
$$w_t = a \left\{ e^{(\sigma x + \alpha t)} w_x \right\}_x + 0.25 w_x, \quad -1 < x < 1, \quad 0 < t \leq 1.0,$$
$$w(x, 0) = e^{3x} \sin^2(3\pi x), \quad -1 \leq x \leq 1, \quad w(-1, t) = w(1, t) = 0, \quad t \geq 0.$$

The initial data $w_0^{red}(x)$ in (19) is shown as the red trace in Figure 4 (bottom), while the computed approximation $f(x)$ to $w^{red}(x, 1)$ is shown as the black trace in the same figure. Using $f(x)$ in (14), the Van Cittert procedure was applied for 650 iterations and resulted in $h^{650}(x) = w_0^{green}(x)$, shown as the green trace in Figure 4 (bottom), with a final L^∞ residual of 1.8E-2, and an L^2 relative error at $t = 1$ of 0.58%. The behavior of $\log \{\| f - S[h^n] \|_\infty\}$ versus n, is shown in Figure 4 (top). Here, $\| w_0^{red} \|_2 = 3.3$, while $\| w_0^{green} \|_2 = 4.7$. Therefore, both solutions $w^{red}(x, t)$ and $w^{green}(x, t)$ in Example 3 satisfy

(20) $\| w(., 1) - f \|_2 \leq \delta \leq 0.0058 \| f \|_2,$ $\| w(., 0) \|_2 \leq M = 4.7.$

Again, even though it is substantially different from $w_0^{red}(x)$, $w_0^{green}(x)$ must be considered a valid reconstruction of the initial data corresponding to the given data $f(x)$ at $t = 1$. The traces for $w^{red}(x, 1)$ and $w^{green}(x, 1)$ are plotted in Figure 5, and are again visually indistinguishable. Indeed, in Figure 5, the green trace was artificially raised by 0.025 so as to render the red trace visible. Here again, the given data $f(x)$ is a close approximation to two very distinct solutions of the parabolic problem in (19). In this example, if it is known a-priori that the initial values must be non negative, this knowledge can be used to reject $w_0^{green}(x)$ as false. Such knowledge would not have been helpful in Example 2.

Behavior of Van Cittert residual norm in Example 3
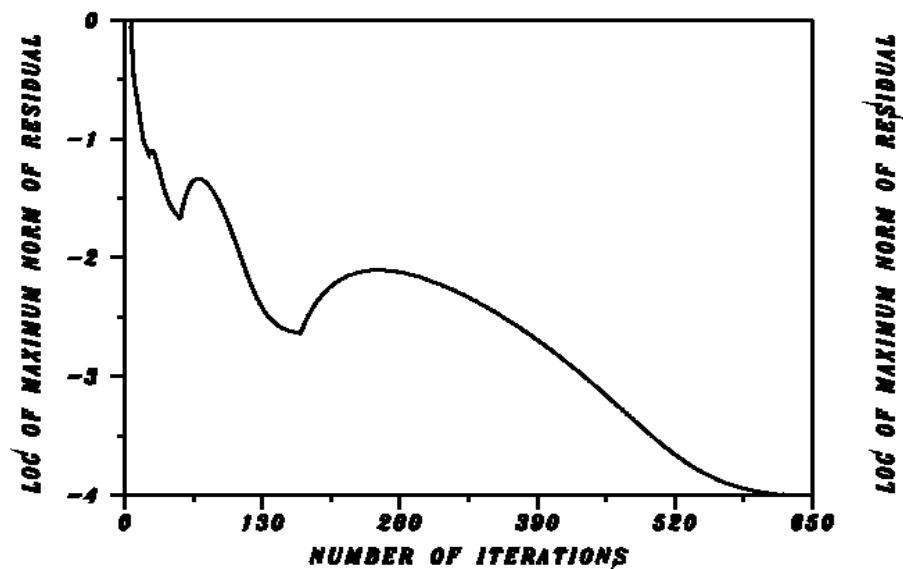
Effective backward non uniqueness in Example 3
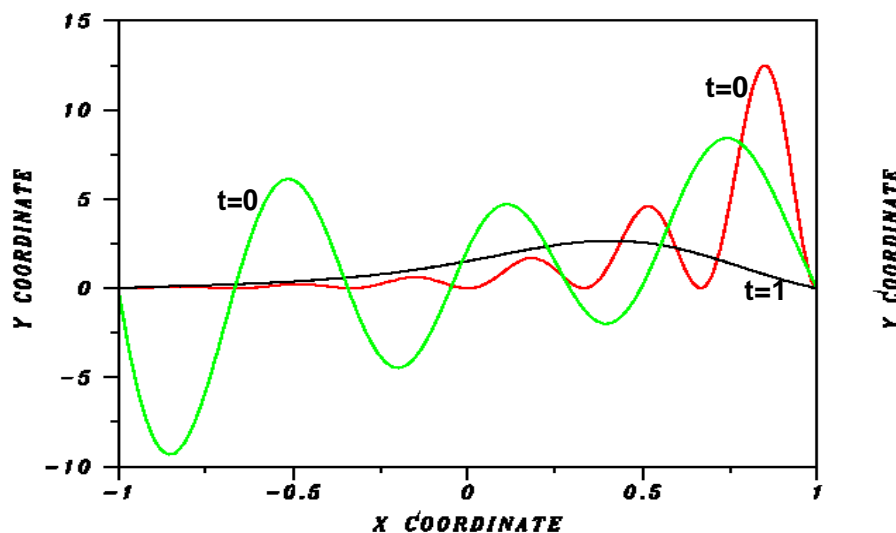
**Either red or green initial values at t=0, terminate on black curve
at t=1 to within 1.8E–2 pointwise, and L2 relative error=5.8E–3.**

FIG. 4. *TOP. Behavior of* $log\{\| f - S[h^n] \|_\infty\}$ *versus iteration number n, in Van Cittert procedure in Example 3. BOTTOM. Ill behavior in non self adjoint problem. Data $f(x)$ (black curve), approximating solution $w^{red}(x,t)$ at time $t = 1$ with an L^2 relative error of 0.58%, recovers strikingly different initial value $w_0^{green}(x)$, in lieu of true initial value $w_0^{red}(x)$.*

Red and green traces at t=1 coincide in Example 3
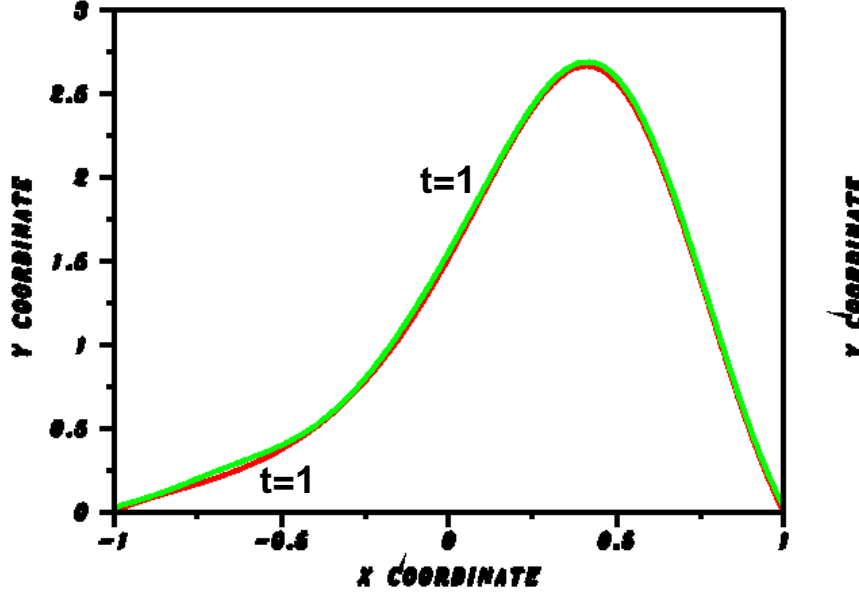
**Green trace artificially raised to render red trace visible.**

FIG. 5. *Red and green traces are the solutions at time $t = 1$, $w^{red}(x, 1)$, $w^{green}(x, 1)$, corresponding to the initial values $w_0^{red}(x)$, $w_0^{green}(x)$, in Figure 4 (bottom). Traces at $t = 1$ agree to within $1.8E - 2$, pointwise. This close agreement explains the difficulty of recovering $w_0^{red}(x)$ from approximate values for $w^{red}(x, 1)$ in Example 3.*

8. Example 4 (Fig. 6). Burgers equation. Behavior in this instructive nonlinear example involving Burgers equation needs to be compared with Example 1 to be fully appreciated. With $a = \alpha = 0.05$, consider

$$w_t = a(w_x)_x - ww_x, \quad -1 < x < 1, \quad 0 < t \leq 1.0,$$
(21)
$$w(x, 0) = e^{2x}\sin(2\pi x), \quad -1 \leq x \leq 1, \quad w(-1, t) = w(1, t) = 0, \quad t \geq 0.$$

The initial value $w_0^{red}(x)$ in (21) is shown as the red trace in Figure 6 (bottom), while the computed approximation $f(x)$ to $w^{red}(x, 1)$ is shown as the black trace in the same figure. The red and black traces in Figure 6 (bottom) bear much the same qualitative and quantitative relationships to each other that occur in the corresponding traces in Figure 1. Using $f(x)$ in (14), the Van Cittert procedure was applied for $40,000$ iterations, resulting in a final L^∞ residual of 7.8E-6, and an L^2 relative error at $t = 1$ of 0.00122%. The behavior of $\log\{\|f - S[h^n]\|_\infty\}$ versus n, is shown in Figure 6 (top). Clearly, $S[h^{40,000}(x)]) = w^{green}(x, 1)$ is a very accurate match to the given data $f(x)$ and to $w^{red}(x, 1)$. However, even with such small residuals, $h^{40,000}(x) = w_0^{green}(x)$, shown as the green trace in Figure 6 (bottom), differs markedly from $w_0^{red}(x)$. The two traces have comparable L^2 norms with $\|w^{red}(., 0)\|_2 = 1.8$ and $\|w^{green}(., 0)\|_2 = 2.2$. Evidently, $w^{green}(x, 1)$ and $w^{red}(x, 1)$ are extremely close together and significantly more accurate data $f(x)$ might be needed to reconstruct the correct initial value $w_0^{red}(x)$. Such accuracy is highly unlikely in practice. This is

Behavior of Van Cittert residual norm in Example 4
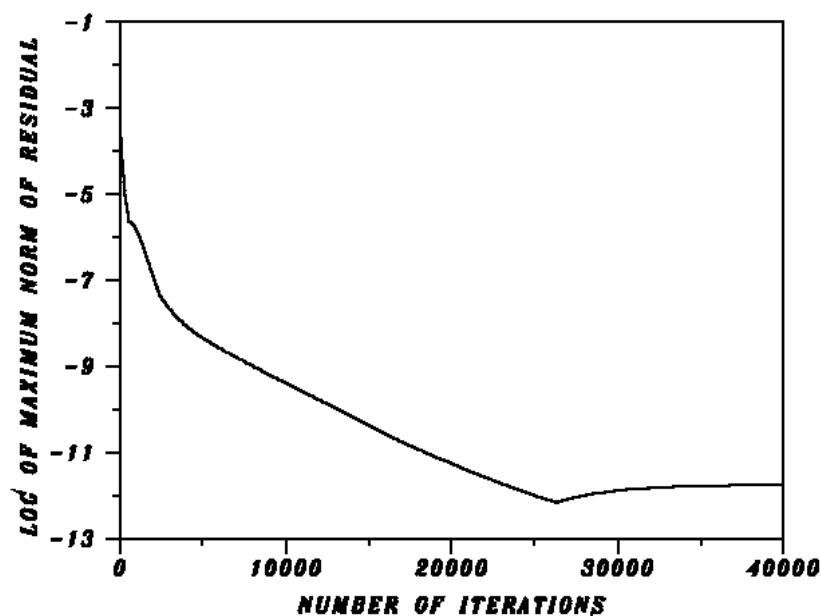
Effective backward non uniqueness in Example 4
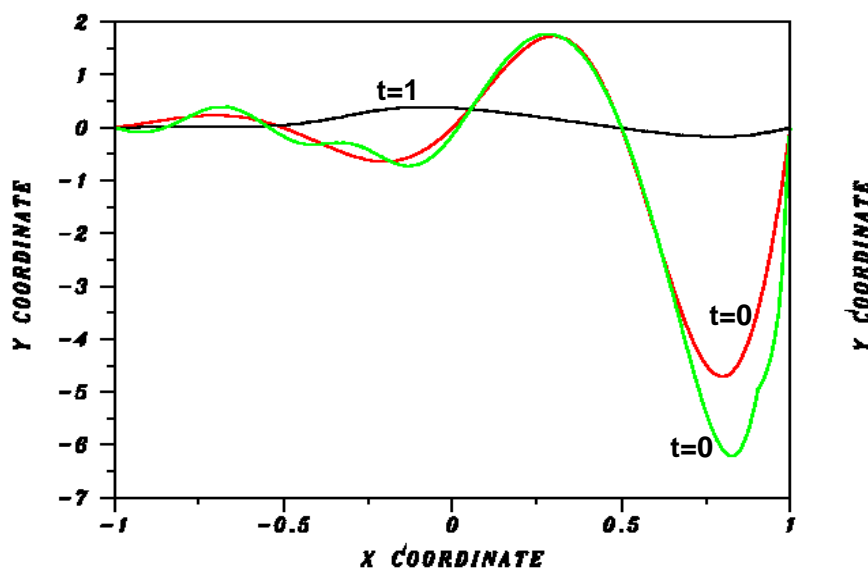
**Either red or green initial values at t=0, terminate on black curve
at t=1 to within 7.8E–6 pointwise, and L2 relative error =1.22E–5.**

FIG. 6. *TOP. Behavior of* $log\,\{\|\,f - S[h^n]\,\|_\infty\}$ *versus iteration number n, in Van Cittert procedure in Example 4. BOTTOM. Intractable recovery in nonlinear Burgers equation. Highly accurate data $f(x)$ (black curve), approximating solution $w^{red}(x,t)$ at time $t = 1$ with an L^2 relative error of 0.00122%, fails to recover true initial value $w_0^{red}(x)$, and results in different initial value $w_0^{green}(x)$. Compare with self adjoint behavior in Figure 1.*

in sharp contrast to Figure 1, where, with a 400 times larger L^∞ residual of 3.1E-3, the reconstructions $w_0^{red}(x)$ and $w_0^{green}(x)$ are reasonably comparable. Clearly, accurate backward recovery can be intractable in some nonlinear parabolic equations.

9. Example 5 (Figs. 7 and 8). Strongly nonlinear. We now consider parabolic equations where the diffusion coefficient is a nonlinear function of the solution,

(22)
$$w_t = 0.05(e^{0.4w}w_x)_x, \quad -1 < x < 1, \quad 0 < t \le 1.0,$$

$$w(x,0) = e^{3x}\sin(2\pi x), \quad -1 \le x \le 1, \quad w(-1,t) = w(1,t) = 0, \quad t \ge 0.$$

The initial data $w_0^{red}(x)$ in (22) is shown as the red trace in Figure 7 (bottom), while the computed approximation $f(x)$ to $w^{red}(x,1)$, is shown as the black trace in the same figure. Using $f(x)$ in (14), the Van Cittert procedure was applied for 750 iterations, resulting in a final L^∞ residual of 2.6E-2, and an L^2 relative error at $t = 1$ of 0.38%. This relative error is smaller than was the case in the well-behaved Example 1. The function $h^{750}(x) = w_0^{green}(x)$ is the green trace in Figure 7 (bottom). The behavior of $\log\{\| f - S[h^n] \|_\infty\}$ versus n, is shown in Figure 7 (top). Here, $\| w_0^{red} \|_2 = 3.7$, while $\| w_0^{green} \|_2 = 3.9$. Therefore, both solutions $w^{red}(x,t)$ and $w^{green}(x,t)$ in Example 5 satisfy

(23)
$$\| w(.,1) - f \|_2 \le \delta \le 0.0038 \| f \|_2, \qquad \| w(.,0) \|_2 \le M = 3.9.$$

The traces for $w^{red}(x,1)$ and $w^{green}(x,1)$ are plotted in Figure 8 and are again visually indistinguishable. As before, the green trace in Figure 8 was artificially raised by 0.075 so as to render the red trace visible. Evidently, $w_0^{green}(x)$ is a valid reconstruction. Note, however, that $\| w_0^{red} \|_\infty = 10.6$, while $\| w_0^{green} \|_\infty = 23.4$, is more than twice as large. Accurate prior knowledge of the L^∞ norm of $w(x,0)$ in (22), *if available*, might be used to reject $w_0^{green}(x)$ as false.

10. Example 6 (Figs. 9 and 10). Strongly nonlinear. While the level of accuracy in this last example is slightly lower than was the case in the preceding examples, that accuracy is representative of several practical applications. Consider the nonlinear problem with non negative solution

(24)
$$u_t = 0.05(e^{0.5u}u_x)_x + uu_x, \quad -1 < x < 1, \quad 0 < t \le 1.0,$$

$$u(x,0) = e^{3x}\sin^2(3\pi x), \quad -1 < x < 1, \quad u(-1,t) = u(1,t) = 0, \quad t > 0.$$

The initial data $w_0^{red}(x)$ in (24) is shown as the red trace in Figure 9 (bottom), while the computed approximation $f(x)$ to $w^{red}(x,1)$ is shown as the black trace in the same figure. Using $f(x)$ in (14), the Van Cittert iteration is not well-behaved in this example. As shown in Figure 9 (top), the smallest L^∞ residual occurs after 49 iterations and has the value 4.4E-2. This is about ten times larger than was the case in the well-behaved Example 1. The function $h^{49}(x) = w_0^{green}(x)$ is the green trace in Figure 9 (bottom). The corresponding L^2 relative error at $t = 1$, $\| f - S[h^{49}] \|_2 / \| f \|_2 = 2.75\%$. This is about 7 times larger than in Example 1, while remaining acceptable. In this case, the traces for $w^{red}(x,1)$ and $w^{green}(x,1)$, plotted in Figure 10, are naturally distinguishable and there is no need for artificially raising one of these traces to render the other one visible. Nevertheless, the agreeement at $t = 1$ is reasonably close and might well be considered satisfactory in many situations

Behavior of Van Cittert residual norm in Example 5
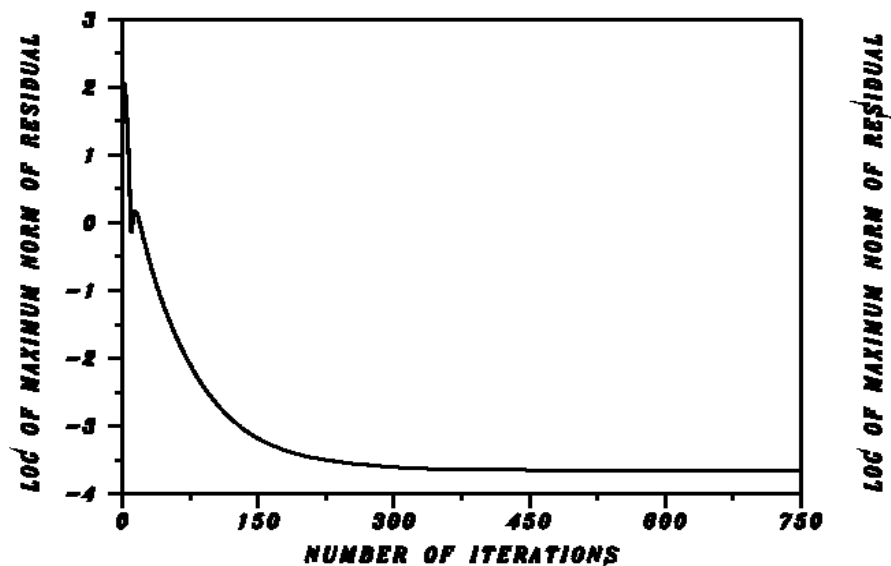
Effective backward non uniqueness in Example 5
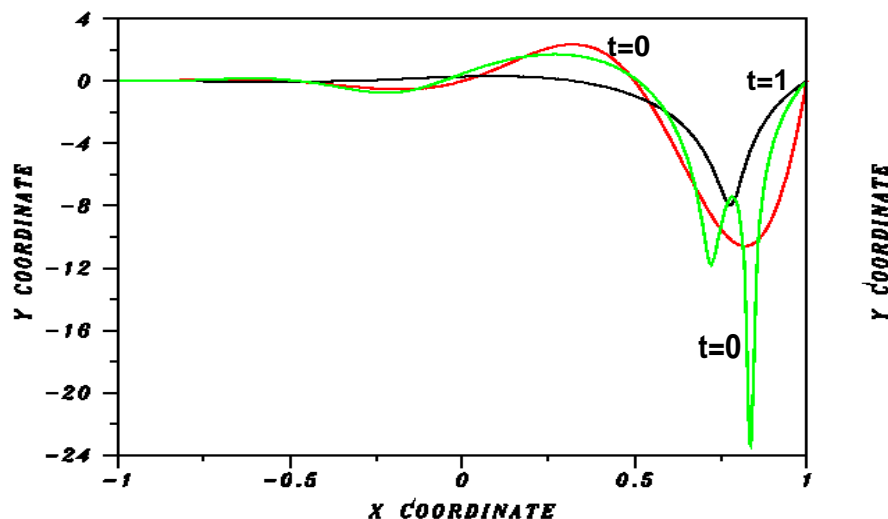
Either red or green initial values at t=0, terminate on black curve at t=1 to within 2.6E–2 pointwise, and L2 relative error=3.8E–3.

FIG. 7. *TOP. Behavior of* $\log\{\| f - S[h^n] \|_\infty\}$ *versus iteration number n, in Van Cittert procedure in Example 5. BOTTOM. Ill behavior in strongly nonlinear problem. Data $f(x)$ (black curve), approximating solution $w^{red}(x,t)$ at time $t = 1$ with an L^2 relative error of 0.38%, recovers substantially different initial value $w_0^{green}(x)$, in lieu of true initial value $w_0^{red}(x)$.*

Red and green traces at t=1 coincide in Example 5

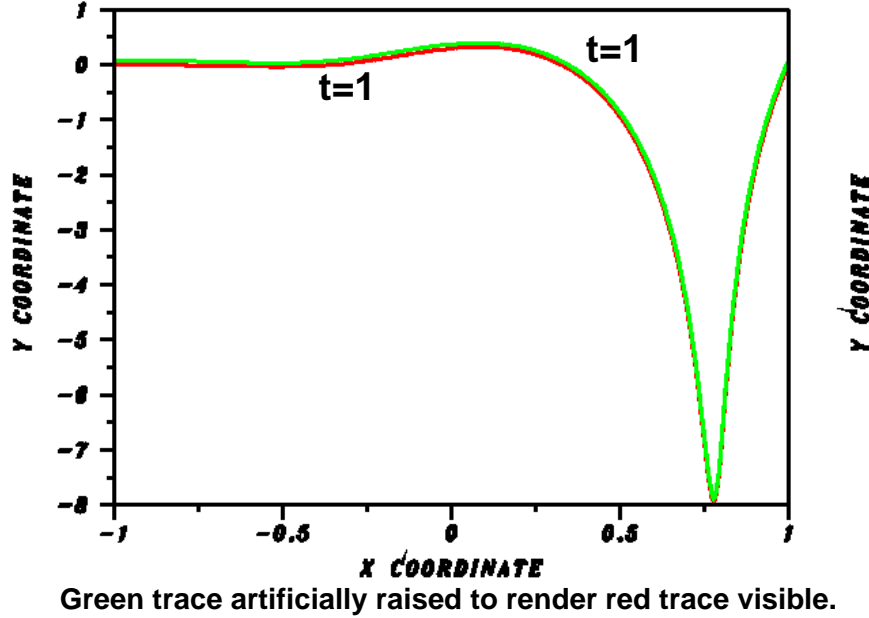**Green trace artificially raised to render red trace visible.**

FIG. 8. *Red and green traces are the solutions at time $t = 1$, $w^{red}(x, 1)$, $w^{green}(x, 1)$, corresponding to the initial values $w_0^{red}(x)$, $w_0^{green}(x)$, in Figure 7 (bottom). Traces at $t = 1$ agree to within $2.6E - 2$, pointwise. This close agreement explains the difficulty of recovering $w_0^{red}(x)$ from approximate values for $w^{red}(x, 1)$ in Example 5.*

involving real data. Moreover, the reconstruction $w_0^{green}(x)$ in Figure 9 (bottom) appears quite plausible. Indeed, given the black trace $f(x)$ in Figure 9 (bottom), the initial value $w_0^{green}(x)$ seems much more likely than $w_0^{red}(x)$. As was the case in Example 2, the beneficial regularizing constraints of smoothness and non negativity, do not eliminate the candidate $w_0^{green}(x)$. In Example 5, accurate prior knowledge of the L^∞ norm at $t = 0$, rather than the L^2 norm, could be used to reject $w_0^{green}(x)$. The reverse is true in the present case. Both green and red curves have an L^∞ norm of about 13. However, $\| w_0^{red} \|_2 = 3.3$, while $\| w_0^{green} \|_2 = 9.7$.

11. Concluding remarks. In recent years, there has been considerable interest in the numerical computation of ill-posed inverse problems, as a result of growth in such fields as non destructive evaluation, geophysical prospecting, remote sensing, diagnostic imaging in medical and industrial applications, and other related areas. One central question, that of stabilizing ill-posed computations so as to prevent explosive noise amplification, has received much attention. This is the regularization problem, which has spawned a large literature.

The problem discussed in this paper is unrelated to such noise amplification, but is equally serious. While backward uniqueness of solutions holds true for large classes of linear and nonlinear parabolic equations, the exact, highly restricted data at time $t = 1$ necessary to recover a particular solution, is seldom available. One must rely on approximate data. However, such data may unexpectedly approximate several

Behavior of Van Cittert residual norm in Example 6
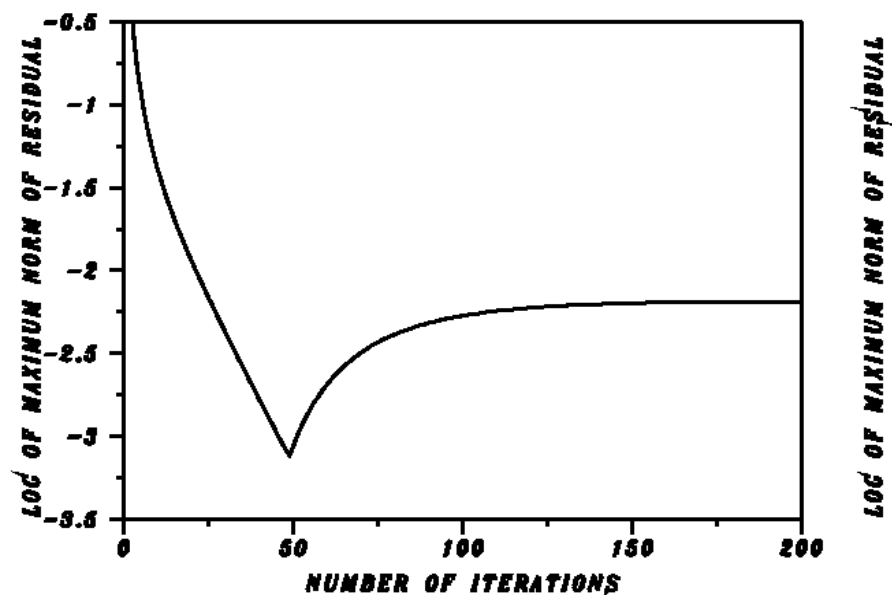
Effective backward non uniqueness in Example 6
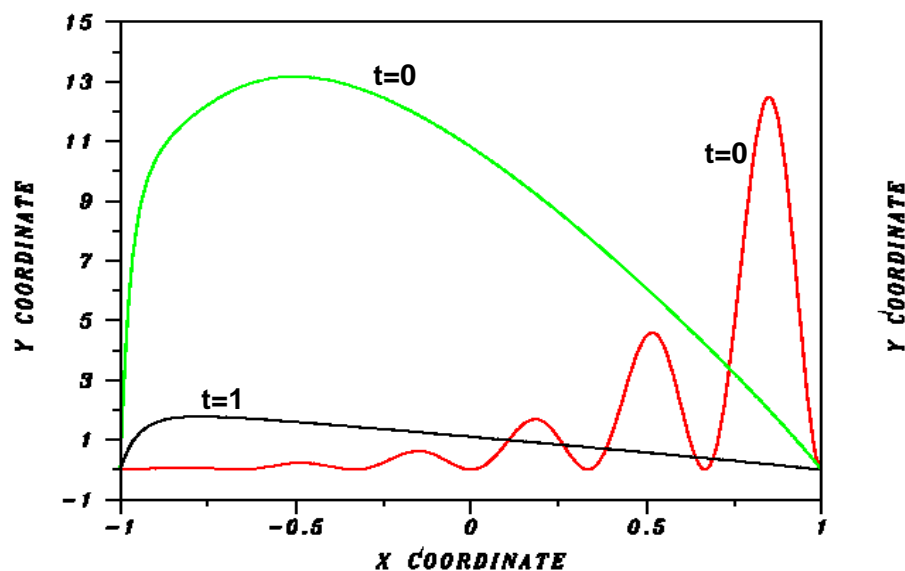
**Either red or green initial values at t=0, terminate on black curve
at t=1 to within 4.4E–2 pointwise, and L₂ relative error=2.75E–2.**

FIG. 9. *TOP. Ill behavior of $\log\{\| f - S[h^n] \|_\infty\}$ versus iteration number n, in Van Cittert procedure in Example 6. BOTTOM. Use of less accurate data in strongly nonlinear problem. Data $f(x)$ (black curve), approximating solution $w^{red}(x,t)$ at time $t = 1$ with an L^2 relative error of 2.75%, recovers plausible, but vastly different initial value $w_0^{green}(x)$, in lieu of true initial value $w_0^{red}(x)$.*

Small deviation in red and green traces in Ex 6
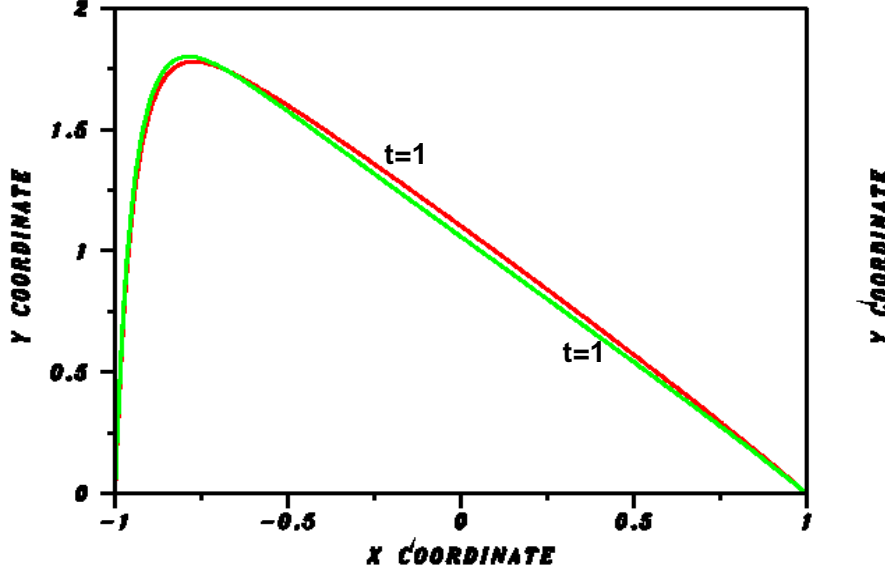
Red and green solutions at t=1 in reasonably good agreement.

FIG. 10. *Red and green traces are the solutions at time* $t = 1$, $w^{red}(x, 1)$, $w^{green}(x, 1)$, *corresponding to the initial values* $w_0^{red}(x)$, $w_0^{green}(x)$, *in Figure 9 (bottom). Traces at* $t = 1$ *agree to within* $4.4E - 2$, *pointwise. This reasonably close agreement explains the difficulty of recovering* $w_0^{red}(x)$ *from approximate values for* $w^{red}(x, 1)$ *in Example 6.*

distinct solutions at time $t = 1$.

This paper has focused attention on a class of 1D parabolic equations $w_t = Lw$, and presented several examples where there is strong computational evidence for the *existence* of distinct solutions $w^{red}(x, t)$ and $w^{green}(x, t)$ on $0 \leq t \leq 1$, having the following properties:

- The quantity $\parallel w^{red}(., 1) - w^{green}(., 1) \parallel_\infty$ is small enough that the traces $w^{red}(x, 1)$ and $w^{green}(x, 1)$ at $t = 1$ are visually indistinguishable.

- The L^2 relative error at $t = 1$, $\left\{ \parallel w^{red}(., 1) - w^{green}(., 1) \parallel_2 / \parallel w^{red}(., 1) \parallel_2 \right\}$ is generally less than 1%.

- The functions $w^{red}(x, 0)$ and $w^{green}(x, 0)$ are smooth, well-behaved, physically plausible, and entirely different. Except in the case of Example 6, both functions have very comparable L^2 norms.

In these examples, there is effective non uniqueness in the recovery of $w^{red}(x, 0)$ in the stabilized backward problem (4), (5), because reasonably accurate data $f(x)$ for the unknown $w^{red}(x, 1)$ also approximates $w^{green}(x, 1)$. Indeed, in Examples 2 and 6, $w^{green}(x, 0)$ appears significantly more compatible with $f(x)$ than does $w^{red}(x, 0)$.

The Van Cittert iterative procedure was a vital part of this investigation. While that iteration seldom converges, and can behave unpredictably and even diverge in some cases, it is able to generate unexpected, valid, noise free, candidate solutions $w^{green}(x,t)$. Other iterative procedures might be found that produce further viable, yet distinctly different, initial functions $w(x,0)$ from the same data $f(x)$. Such multiple possible solutions explain why the inequality (13) does not guarantee any accuracy at $t = 0$, but only provides the redundant information $\parallel w^1(.,0) - w^2(.,0) \parallel_2 \leq 2M$. To the author's knowledge such explicit examples of effective non uniqueness are new.

The Hölder exponent $\mu(t)$ in the inequality (13) also plays an important behind the scenes role in the above examples. That exponent is a property of the particular parabolic equation, and it reflects how fast that equation forgets the past. It may be viewed as a barometer on the difficulty of backward reconstruction. The relatively well-behaved self adjoint problem in Example 1, corresponds to the best possible case where $\mu(t) = t$. However, as shown in [13], non self adjointness, nonlinearity, and other adverse properties of the elliptic spatial operator L in (4), can cause significantly faster decay of $\mu(t)$ to zero, as $t \downarrow 0$. Behavior in the non self adjoint Examples 2 and 3 illustrate this point. The intractable recovery in the Burgers equation in Example 4 is especially noteworthy.

These unexpected results imply a need for caution in applying backward parabolic equations. There is ever growing interest in the use of backward parabolic equations as an all-purpose image sharpening tool. Images blurred by space variant, non isotropic, Gaussian like point spread functions, are equivalent to solutions of 2D linear non self adjoint parabolic equations, with variable coefficients. Examples 2 and 3 imply that false deblurred images are possible from approximately known blurred image data, even with very little noise. Likewise, the 2D or 3D advection dispersion equation could potentially generate false backward solutions from reasonably accurate knowledge of the current contaminant spatial distribution.

REFERENCES

[1] K. A. AMES AND B. STRAUGHAN, *Non-standard and Improperly Posed Problems*, Academic Press, New York, 1997.

[2] K. A. AMES AND J. F. EPPERSON, *A kernel-based method for the approximate solutions of backward parabolic problems*, SIAM J. Numer. Anal., 34 (1997), pp. 1357–1390.

[3] J. ATMADJA, *The Marching-jury Backward Beam Equation Method And Its Application To Backtracking Non-reactive Plumes In Groundwater*, PhD Dissertation, (2001), Columbia University.

[4] J. ATMADJA AND A. C. BAGTZOGLOU, *Pollution source identification in heterogeneous porous media*, Water Resources Research, 37 (2001), pp. 2113-2125. DOI 10.1029/2001WR000223

[5] A. C. BAGTZOGLOU AND J. ATMADJA, *Marching-jury backward beam equation and quasi-reversibility methods for hydrologic inversion: Application to contaminant plume spatial distribution recovery*, Water Resources Research, 39 (2003), pp. 1038–1052. DOI 10.1029/2001WR001021.

[6] A. C. BAGTZOGLOU AND J. ATMADJA, *Mathematical methods for hydrologic inversion: The case of pollution source identification*, Handb Environ Chem Vol. 5, Part F,Vol. 3 (2005): pp. 6596. DOI 10.1007/b11442.

[7] S. A. BAUN AND A. C. BAGTZOGLOU, *A computationally attractive approach for near real-time contamination source identification*, Developments in Water Science, 55 (2004), pp. 1263-1271. DOI 10.1016/S0167-5648(04)80141-2

[8] M. BERZINS AND P. M. DEW, *Algorithm 690: Chebyshev polynomial software for elliptic-parabolic systems of PDEs*, ACM Trans. Math. Software, 17 (1991), pp. 178–206.

[9] B. L. BUZBEE AND A. S. CARASSO, *On the numerical computation of parabolic problems for preceding times*, Math. Comp., 27 (1973), pp. 237-266.

[10] J. R. CANNON, *Some numerical results for the solution of the heat equation backwards in time*,

Proc. Adv. Sympos. Numerical Solutions of Nonlinear Diffferential Equations (Madison, WI 1966), pp. 21–54. Wiley, New York, 1966.

[11] A. S. Carasso, *Overcoming Hölder continuity in ill-posed continuation problems*, SIAM J. Numer. Anal., 31 (1994), pp. 1535–1557.

[12] A. S. Carasso, *Linear and nonlinear image deblurring: a documented study*, SIAM J. Numer. Anal., 36 (1999), pp. 1659–1689.

[13] A. S. Carasso, *Logarithmic convexity and the 'slow evolution' constraint in ill-posed initial value problems*, SIAM J. Math. Anal., 30 (1999), pp. 479–496.

[14] A. S. Carasso, *Bochner subordination, logarithmic diffusion equations, and blind deconvolution of Hubble space telescope imagery and other scientific data*, SIAM J. Imaging Sciences, 3 (2010), pp. 954–980.

[15] A. S. Carasso, J. G. Sanderson and J. M. Hyman, *Digital removal of random media image degradations by solving the diffusion equation backwards in time*, SIAM J. Numer. Anal., 15 (1978), pp. 343–367.

[16] R. E. Ewing, *The approximation of certain parabolic equations backward in time by Sobolev equations*, SIAM J. Math. Anal., 6 (1975), pp. 283–294.

[17] H. Han, M. Yan, and C. Wu, *An energy regularization method for the backward diffusion problem and its applications to image deblurring*, Commun. Comput. Phys., 4 (2008), pp. 177–194.

[18] P. A. Jansson, *Deconvolution with Application in Spectroscopy*, Academic Press, New York, 1984.

[19] W. Höhn, *Finite elements for parabolic equations backwards in time*, Numer. Math., 40 (1982), pp. 207–227.

[20] R. J. Knops, *Logarithmic convexity and other techniques applied to problems in continuum mechanics*, in Symposium on Non-Well-Posed Problems and Logarithmic Convexity, R. J. Knops, ed., Lecture Notes in Math. 316, Springer-Verlag, New York, 1973.

[21] R. J. Knops and L. E. Payne, *On the stability of solutions of the Navier-Stokes equations backward in time*, Arch. Rat. Mech. Anal., 29 (1968), pp. 331–335.

[22] R. L. Lagendijk and J. Biemond, *Iterative Identification and Restoration of Images*, Kluwer Academic Publishers, Boston, 1991.

[23] R. Lattès and J. L. Lions, *The Method of Quasi-Reversibility*, American Elsevier, New York, 1969.

[24] C.-S. Liu, *An efficient backward group preserving scheme for the backward in time Burgers equation*, Comput Model Eng Sci, 12 (2006), pp. 5565.

[25] C.-S. Liu, C.-W. Chang, and J.-R. Chang, *The backward group preserving scheme for 1D backward in time advection-dispersion equation*, Numerical Methods for Partial Differential Equations, 26 (2008), pp. 6180.

[26] J. Lee and D. Sheen, *A parallel method for backward parabolic problems based on the Laplace transformation*, SIAM J. Numer. Anal. 44 (2006), pp. 1466–1486.

[27] J. Lee and D. Sheen, *A parallel method for backward parabolic problems and its application to image deblurring: Part II*. See http://www.ksiam.org/conference/annual061/upfile/ksiam-submit.pdf (2006). pp. 41–54.

[28] J. M. Marbán and C. Palencia, *A new numerical method for backward parabolic problems in the maximum-norm setting*, SIAM J. Numer. Anal., 40 (2002), pp. 1405–1420.

[29] R. M. Neupauer and J. L. Wilson, *Backward probabilistic model of groundwater contamination in non-uniform and transient flow*, Advances in Water Resources, 25 (2002) pp. 733-746.

[30] L. E. Payne, *Improperly Posed Problems in Partial Differential Equations*, CBMS-NSF Regional Conference Series in Applied Mathematics, Volume 22 (1975), SIAM Publications, Philadelphia, PA.

[31] T. H. Skaggs and Z. J. Kabala, *Recovering the history of a groundwater contaminant plume: Method of Quasi-Reversibility*, Water Resources Research, 31 (1995), pp. 2669–2673. DOI 10.1029/95WR02383

[32] N. H. Tuan and D. D Trong, *A nonlinear parabolic equation backward in time: Regularization with new error estimates*, Nonlinear Analysis: Theory, Methods and Applications, 73 (2010), pp. 1842–1852. DOI 10.1016/j.na.2010.05.019

[33] L. Wang, S. Luo, and Z. Wang, *Image deblur with regularized backward heat diffusion*, Image Processing (ICIP), 2010 17th IEEE International Conference Proceedings, pp. 1141–1144. DOI 10.1109/ICIP.2010.5651365